Low Complexity Performance Assessment of a Sensor Array via Unscented Transformation

Ricardo Kehrle Miranda[1,2,*], João Paulo C. L. da Costa[1,2,3], Florian Roemer[3], Leonardo R.A.X. Menezes[1], Giovanni Del Galdo[2,3], André L. F. de Almeida[4]

rickehrle@unb.br, joaopaulo.dacosta@ene.unb.br, florian.roemer@tu-ilmenau.de, leonardo@ene.unb.br, giovanni.delgaldo@tu-ilmenau.de, andre@gtel.ufc.br

[1]*Department of Electrical Engineering, University of BrasÃηlia, Brasília-DF, Brazil,* [2]*Institute for Information Technology, Ilmenau University of Technology, Ilmenau, Germany,* [3]*Fraunhofer Institute for Integrated Circuits IIS, Erlangen, Germany,* [4]*Department of Teleinformatics Engineering, Federal University of Ceará, Fortaleza, Brazil*

Abstract

Due the advances on electronics, applications of antenna array signal processing are becoming more frequent. When employing antenna arrays for beamforming, the signal to interference and noise ratio (SINR) should be assessed. Many factors can affect the SINR such as the array element positioning error and the direction of arrival (DOA) estimation error. In these cases, the assessment is traditionally performed via the SINR average obtained using Monte Carlo (MC) simulations. However, this approach requires a great amount of realizations that demand a high computational effort and processing time due to its slow convergence. In this paper, we propose a low complexity performance assessment of the average SINR via unscented transformation. Compared to MC simulations, our proposed method requires only a few trials and has a negligible computational complexity, yet giving a comparable SINR when the DOA estimation is perturbed. When the antenna elements positioning is perturbed, a multivariate scenario arises. For multivariate scenario the proposed scheme has an exponential increase in complexity, therefore, still being advantageous for a small number of antennas.

Keywords: sensor array, SINR, unscented transformation, Monte Carlo

*Corresponding author

simulation, beamforming

1. Introduction

Applications such as speech and audio acquisition [1, 2], wireless communications [3] and RADAR [4] make use of array signal processing in order to enhance their capabilities. One of the most common uses of antenna arrays is spatial filtering by the use of beamformers [5]. However, idealistic assumptions such as a known direction of arrival (DOA) of the desired signal or perfectly spaced array elements are usually made [6]. Therefore, a performance assessment in the presence of deviations should be considered for practical implementations.

Geometry based beamformers, e.g. delay and sum (DS), generalized sidelobe cancellers (GSC) and minimum variance distortionless response (MVDR), take one or more DOAs as input parameters of the associated optimization problem. Though, DOA estimation is always prone to a certain degree of error. Moreover, the positioning of the antenna elements is not always perfectly known and it may affect the beamformer's quality. In this paper, the quality is measured as the average of the achieved signal to interference and noise ratio (SINR). The average is important, since the random nature of these perturbations will lead to random SINR values that may cause inconclusive results. For example, simulation in a more favorable scenario may result in an SINR that is lower than that of a simulation in a less favorable one. However, these values vary around a mean and computing the average gives the system designer an overall SINR, i.e. which SINR level one expects to get when the system is subject to a certain degree of error.

The Monte Carlo (MC) method [7] is a commonly used simulation technique for the computation of the average SINR [8] due to its simplicity and easiness of implementation. However, it requires a large number of trials [9] to converge to a satisfactory result, implying a long simulation time. Currently, performance assessment of embedded systems takes 30 % of the development time and it could increase to 70 % [10]. Therefore, improving the efficiency of performance

assessment tools implies reducing production costs and delivering new solutions faster to the market.

Previous works derive analytical expressions to assess the system's quality by using first order expansions of the perturbed parameters [11, 12]. These analytical expression evaluate the perturbation due to noise and are exact for high signal to noise ratio (SNR) values, but they do not present a good fit for low SNR cases. In this paper, we study the effect of other type of perturbations, more precisely the DOA estimation error and antenna element positioning error on the SINR. We show that, in these cases, the computation of such analytical expressions is hard or not practical and we propose the use of the unscented transformation (UT) to numerically evaluate the SINR. The UT maps a continuous probability distribution into a discrete one with the same statistical moments [13]. When a non-linear function is applied to the mapped distribution, in our case the SINR function, the results give us a good fit in comparison to the traditional MC approach, yet with a negligible computational time for univariate perturbation models. When the perturbation is multivariate, e.g. error in the position of each antenna element, the complexity grows exponentially with the number of antennas. Therefore, the complexity is still lower than the MC method's complexity for a small number of antennas and greater for a large number of antennas. In order to alleviate the effect of the array spacing perturbation using the UT, the reader is referred to [14].

In this work we consider two perturbations, a DOA estimation error and array element positioning error. The evaluation of these perturbations give raise to a univariate and multivariate UT, respectively. For the sake of demonstration, one type of perturbation is considered for each case. In future work, the UT may also be applied for other types of perturbations such as frequency shift, mutual coupling, amplitude error and phase error. Also, other integration methods such as the quadrature and cubature transforms [15] showed better results than the UT for filtering purposes. Even though the quadrature and cubature transforms might also be considered for sensor array performance assessment, we regard them as future work and focus on the simplicity and ease of implementation of

the UT.

The remainder of this paper is divided as follows. Section 2 shows the data model containing the considered perturbations. In Section 3, we overview basic concepts of the UT. In Section 4, we propose the performance assessment of a beamformer using the UT. Section 5 presents the simulations results. Finally, Section 6 draws the conclusions of this work.

2. Data Model

We start with the received signal model of an ideal uniform linear array (ULA) containing M antenna elements

$$\mathbf{x}(t) = \sum_i \mathbf{a}(\theta_i) s_i(t) + \mathbf{v}(t) \in \mathbb{C}^{M\times 1}, \tag{1}$$

where $\mathbf{a}(\theta_i)$ is the steering vector, θ_i is the DOA azimuth of i-th source signal $s_i(t)$ and $\mathbf{v}(t)$ is the additive noise term. Since we are dealing with a ULA, the steering vector contains the phase delays $a_{m,i} = e^{j2\pi\mu_i}$, where $\mu_i = (m-1)\frac{d}{\lambda}\cos\theta_i$, m is the antenna element index and d is the inter-element spacing in wavelengths. If d is given in wavelengths, the wavelength can be dropped from the phase delay μ_i.

Let us consider the case where DOA and element positioning errors are present as depicted in Figure 1.

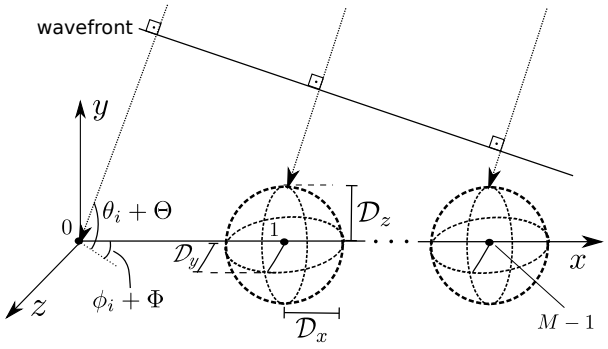

Figure 1: Illustration of a plane wavefront impinging on an antenna array containing DOA and element positioning errors

Figure 1 shows that a plane wavefront reaches the ULA with a DOA angle θ_i and is subject to an additive deviation represented by the Gaussian distributed random variable $\Theta \sim \mathcal{N}(0, \sigma_\theta^2)$. Therefore, the received signal in the presence of DOA estimation error becomes:

$$\mathbf{x}^{(\Theta)}(t) = \mathbf{a}^{(\Theta)}(\theta_0)s_0(t) + \sum_{i\neq 0} \mathbf{a}(\theta_i)s_i(t) + \mathbf{v}(t) \in \mathbb{C}^{M\times 1}, \tag{2}$$

where $\mathbf{a}^{(\Theta)}(\theta_0) = \mathbf{a}(\theta_0+\Theta)$ is the steering vector perturbed by a random variable Θ and the signal of interest (SOI) corresponds to the $i = 0$ source signal. Note that (2) models the DOA estimation error as a physical change in the signal's direction.

Also, in Figure 1, the solid dots represent the antenna element positions. The first element is the reference of the Cartesian axes. The remaining elements are positioned at $(m-1)d$ along the x axis. Each of the elements, except the reference element, is subject to a positioning error in all of the 3 space dimensions x, y and z and are modeled by the random variables $\mathcal{D}_x$, $\mathcal{D}_y$ and $\mathcal{D}_z$, respectively.

When the three dimensions are considered, not only the azimuth θ_i of the DOA, but also its elevation ϕ_i matters. Expanding the phase delays for the three dimensions we obtain

$$\begin{aligned}\mu_{m,i} =&(m-1)d\cos\theta_i\cos\phi_i + \mathcal{D}_{x,m}\cos\theta_i\cos\phi_i \\ &+ \mathcal{D}_{y,m}\sin\theta_i\cos\phi_i + \mathcal{D}_{z,m}\sin\phi_i,\end{aligned} \tag{3}$$

where the subscript m indicates the antenna index, since the random variables are independent with respect to each other.

The received signal for a random array positioning can be written as

$$\mathbf{x}^{(\boldsymbol{\mathcal{D}})}(t) = \sum_i \mathbf{a}^{(\boldsymbol{\mathcal{D}})}(\theta_i, \phi_i)s_i(t) + \mathbf{v}(t) \in \mathbb{C}^{M\times 1}, \tag{4}$$

where $\mathbf{a}^{(\boldsymbol{\mathcal{D}})}(\theta_i, \phi_i) = [e^{j\mu_{1,i}}, e^{j\mu_{2,i}}, \ldots, e^{j\mu_{M,i}}]^{\mathrm{T}}$ is the steering vector perturbed by the random vector

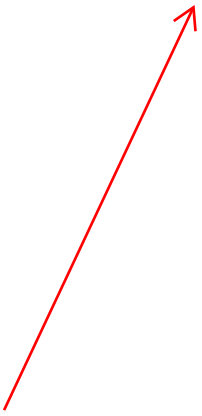

$$\boldsymbol{\mathcal{D}} = [\mathcal{D}_{x,1}, \mathcal{D}_{y,1}, \mathcal{D}_{z,1}, \mathcal{D}_{x,2}, \ldots, \mathcal{D}_{z,M}].$$

3. Unscented Transformation

The Unscented Transformation (UT) is based on the mapping of a continuous probability distribution into a discrete one and can be used to compute the moments of non-linear transformations of a random variable [16]. Traditionally, such moments are computed via MC simulations. However, this approach requires large computational efforts and, depending on the accuracy, the computational complexity can be prohibitive.

In this section we review th cepts of the UT. The UT for a single random variable is reviewed in Subsection 3.1 and its extension for multiple i.i.d. random variables is reviewed in Subsection 3.2, respectively.

3.1. Univariate UT

Let us define the k-th moment of a continuous distribution [17]

$$\mu^{(\kappa)} = \mathrm{E}\{U^{\kappa}\} = \int_{-\infty}^{\infty} f_U(u) u^{\kappa} du, \tag{5}$$

where $f_U(u)$ is the probability density function (PDF) of the random variable U. Then, we make a discrete approximation of $f_U(\cdot)$,

$$f_U(u) \approx \omega(p_n) = \sum_n \omega_n \delta(u - p_n), \tag{6}$$

where p_n are the UT sigma points, ω_n are the weights and $\delta(u)|_{u=0} = 1$ and $\delta(u) = 0$ for any other values of u. Using (6), we write the discrete version of (5) [18]:

$$\hat{\mu}_{\mathrm{ut}}^{(\kappa)} = \sum_n \omega_n p_n^{\kappa}, \tag{7}$$

To summarize, $\omega(p_n)$ is a discrete approximation of $f_U(u)$ with value (weight) ω_n at the sigma point p_n. The number of sigma points is chosen in accordance

with the application and the desired accuracy. The weights and sigma points are calculated by solving the nonlinear system generated from the expansion of Equation (7) and by setting different values for κ, as follows:

$$\begin{cases} \omega_1 + \omega_2 + ... = 1 \\ \omega_1 p_1 + \omega_2 p_2 + ... = \mathrm{E}\{U\} \\ \vdots \\ \omega_1 p_1^K + \omega_2 p_2^K + ... = \mathrm{E}\{U^K\}, \end{cases} \tag{8}$$

where K is the highest order used for the computations. The moments are known and the variable K depends on the number of sigma points and the type of distribution, since some moments might be zero for a chosen distribution.

For instance, in the case of a Gaussian random variable with zero mean, we can take advantage of symmetry, i.e. $\omega_1 = \omega_3$, $p_1 = -p_3$ and $p_2 = 0$. Using this symmetry, only 3 moments are needed in order to find the 6 parameters that, once computed, give $p_1 = -p_3 = \sqrt{3}\sigma^2$, $p_2 = 0$, $\omega_1 = \omega_3 = 1/6$ and $\omega_2 = 2/3$. Figure 2 compares a continuous PDF with its approximation using a 3-point UT and a 5-point UT. Note that the increase in UT points translates to better PDF approximation such that the UT with infinite sigma points is equivalent the continuous PDF.

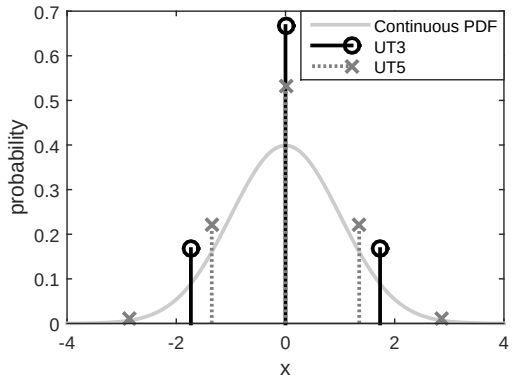

Figure 2: Comparison between a continuous PDF and a 3-point UT and 5-point UT PDF approximation

The mapped points and weights hold the same moments as $f_U(\cdot)$ up to the biggest values used for κ. Therefore, we can replace the mean computed using MC simulation by the UT, i.e. the mean of a non-linear function of a random variable [18]

$$\mathrm{E}\big\{g(U)\big\} = \sum_n \omega_n g(p_n), \tag{9}$$

where $g(\cdot)$ is a non-linear function which depends on the application and scenario (in Section 4 we use the SINR function).

The fastest way to acknowledge Equation (9) is to expand $g(U)$ in its Taylor series

$$\begin{aligned}\mathrm{E}\big\{g(U)\big\} =& \mathrm{E}\Big\{g(0) + \left.\frac{dg(u)}{du}\right|_{u=0} u + \frac{1}{2!}\cdot\left.\frac{d^2g(u)}{du^2}\right|_{u=0} u^2 \\ &+ \frac{1}{3!}\cdot\left.\frac{d^3g(u)}{du^3}\right|_{u=0} u^3 + \dots\Big\} \qquad (10)\\ =& \, a_0 + a_1\mathrm{E}\{U\} + a_2\mathrm{E}\{U^2\} + a_3\mathrm{E}\{U^3\} + \dots, \qquad (11)\end{aligned}$$

where a_i is the i-th Taylor series coefficient. Therefore, if the moments (5) and (7) are equal, Equation (9) is exact. However, by computing the UT we are truncating (11) at the K-th moment as defined in (8).

The condition on $g(\cdot)$ is that its derivatives should be continuous. Also note that the probability distribution of the original function is unknown and only its statistical moments are needed to compute the UT.

3.2. Multivariate UT

In the case where multiple random variables are present in the system model, a random vector $\boldsymbol{U} = [U_1, U_2, \dots, U_M]^{\mathrm{T}}$ is considered. For i.i.d. random variables, the expected values of the cross-products are zero. Thus, the expected values of $\boldsymbol{U}$ result in a set of univariate integrals

$$\mathrm{E}[U_1^{\kappa_1}, \dots, U_m^{\kappa_m}, \dots, U_M^{\kappa_M}] = \int_{\mathbb{R}} f_{U_m}(u_m) u_m^{\kappa_m} du_m, \tag{12}$$

where $\kappa_m \in \{1, 2, \dots\}$ and $\kappa_{j \neq m} = 0$. Therefore, computing the UT for i.i.d. random variables simplifies to (8). Also, the expected value of $g(\boldsymbol{U}) : \mathbb{R}^M \to \mathbb{R}$ is expressed as

$$\begin{aligned} \mathrm{E}[g(\boldsymbol{U})] &= \int_{\mathbb{R}^M} f(u_1, u_2, \dots, u_M) g(\mathbf{u}) d\mathbf{u} \\ &= \int_{\mathbb{R}^M} \prod_m f_{U_m}(u_m) g(\mathbf{u}) d\mathbf{u}. \end{aligned} \tag{13}$$

Since the multivariate polynomial can be written as the product of univariate polynomials [19] and by considering that $g(\boldsymbol{U})$ is approximated by a multivariate polynomial, Equation (13) can be easily computed if $\boldsymbol{U}$ is i.i.d. Hence, (13) becomes a product of univariate integrals leading to the final result in Equation (18). However, the polynomial approximation can be dropped by using (6) and the i.i.d. assumption to get the multivariate PDF

$$f_{\boldsymbol{U}}(\boldsymbol{u}) \approx \prod_m \sum_{n_m} \omega_{n_m} \delta(u_m - p_{n_m}). \tag{14}$$

Via (14), $\mathrm{E}[g(\boldsymbol{U})]$ can be evaluated without the polynomial assumption in the following way

$$\mathrm{E}[g(\boldsymbol{U})] \approx \int_{\mathbb{R}^M} g(\boldsymbol{u}) \prod_m \sum_{n_m} \omega_{n_m} \delta(u_m - p_{n_m}) d\mathbf{u} \tag{15}$$

$$= \int_{\mathbb{R}^M} g(\boldsymbol{u}) \sum_{n_1} \cdots \sum_{n_M} \prod_m \omega_{n_m} \delta(u_m - p_{n_m}) d\mathbf{u} \tag{16}$$

$$= \sum_{n_1} \cdots \sum_{n_M} \int_{\mathbb{R}^M} g(\boldsymbol{u}) \prod_m \omega_{n_m} \delta(u_m - p_{n_m}) d\mathbf{u}. \tag{17}$$

Using the multidimensional sifting property in (17), we find the UT mapping for the i.i.d. multiple random variables

$$\mathrm{E}[g(\boldsymbol{U})] \approx \sum_{n_1} \cdots \sum_{n_M} g(\mathbf{p}_{n_1, \dots, n_M}) \left(\prod_m \omega_{n_m} \right), \tag{18}$$

where $\mathbf{p}_{n_1,\ldots,n_M} = [p_{n_1}, \ldots, p_{n_M}]^{\mathrm{T}}$ is the vector of sigma points.

4. Proposed Performance Assessment of Array Response via UT

In this section, we propose a beamforming performance evaluation technique in the presence of DOA and positioning deviations using the UT. For the beamformer we choose the classical Delay and Sum (DS) technique [20]. The DS filter is $\mathbf{w} = \mathbf{a}(\theta_0)$ and our goal is to evaluate the signal to interference plus noise ratio (SINR). The SINR for uncorrelated signals is

$$\mathrm{SINR} = \frac{\mathbf{w}^{\mathrm{H}}\mathbf{R}_{\mathbf{ss}}\mathbf{w}}{\mathbf{w}^{\mathrm{H}}(\mathbf{R}_{\mathrm{int}} + \sigma^2\mathbf{I})\mathbf{w}}, \tag{19}$$

where σ^2 is the white noise variance. For uncorrelated signals, the SOI correlation matrix $\mathbf{R}_{\mathbf{ss}}$ and the interference correlation matrix $\mathbf{R}_{\mathrm{int}}$ become

$$\mathbf{R}_{\mathbf{ss}} = \mathbf{a}(\theta_0)\mathbf{a}^{\mathrm{H}}(\theta_0), \tag{20}$$

$$\mathbf{R}_{\mathrm{int}} = \sum_{i\neq 0} \mathbf{a}(\theta_i)\mathbf{a}^{\mathrm{H}}(\theta_i). \tag{21}$$

The result of inserting perturbations, as modeled in (2) and (4), implies the replacement of $\mathbf{a}(\theta_i)$ for $\mathbf{a}^{(\Theta)}(\theta_i)$ in (20) and (21) for the case where DOA estimation error is considered. When perturbations on the antenna element positions are considered, we replace $\mathbf{a}(\theta_i)$ for $\mathbf{a}^{(\mathcal{D})}(\theta_i)$. From the random nature of $\mathbf{a}^{(\Theta)}(\theta_i)$ and $\mathbf{a}^{(\mathcal{D})}(\theta_i)$, it becomes clear that the SINR is also random. However, it is expected that the random SINR values vary around a mean. This mean can be used as a reference by the system designer to verify the impact of the DOA estimation error and element positioning error on the output SINR. In Sections 4.1 and 4.2, we present the classical MC approach and the proposed UT approach for the computation of the SINR mean. In this paper the averaged SINR will be denoted as $\overline{\mathrm{SINR}}$.

4.1. Univariate case: Evaluating the SINR under DOA estimation error

We first consider the univariate case, i.e. a single DOA estimation error is present. This error is univariate because the same perturbation is equally reflected throughout the elements of $\mathbf{a}_\Theta(\theta_0 + \Theta)$. When the random variable is independent for each element of the steering vector, it is said to be multivariate (see Section 4.2).

The traditional method for evaluating the SINR is to compute the mean of the SINR over several realizations of Θ. The average value is then expressed as:

$$\overline{\mathrm{SINR}}^{(\Theta)}_{\mathrm{MC}} = \frac{1}{N}\sum_{n=1}^{N} \frac{\mathbf{w}^{\mathrm{H}}\mathbf{R}^{(\Theta)}_{\mathbf{ss}}(\Theta[n])\mathbf{w}}{\mathbf{w}^{\mathrm{H}}(\mathbf{R}^{(\Theta)}_{\mathrm{int}}(\Theta[n]) + \sigma^2\mathbf{I})\mathbf{w}}, \tag{22}$$

where $\Theta[n]$ is the n-th realization of Θ, and the resulting correlation matrices are given by:

$$\mathbf{R}^{(\Theta)}_{\mathbf{ss}}(\Theta[n]) = \mathbf{a}(\theta_0 + \Theta[n])\mathbf{a}^{\mathrm{H}}(\theta_0 + \Theta[n]), \tag{23}$$

$$\mathbf{R}^{(\Theta)}_{\mathrm{int}}(\Theta[n]) = \sum_{i\neq 0} \mathbf{a}(\theta_i + \Theta[n])\mathbf{a}^{\mathrm{H}}(\theta_i + \Theta[n]). \tag{24}$$

Note that this average can be very time consuming since it could take thousands of realizations to average the SINR to a reasonable level. In order to reduce the computational burden of such calculations, we propose the use of (9) to average the SINR in a more computationally efficient way. Typically, less than 10 samples need to be generated, reducing drastically the computational time in comparison to MC simulations. With the knowledge of a few first moments of the random variable Θ, we deterministically compute the UT weights and sigma points as described in Section 3. The UT average of the SINR is obtained by replacing $g(\cdot)$ in Equation (9) by the SINR and Θ_n by $p_n^{(\Theta)}$:

$$\overline{\mathrm{SINR}}^{(\Theta)}_{\mathrm{UT}} = \sum_{n=1}^{N_{\mathrm{UT}}} \omega_n \frac{\mathbf{w}^{\mathrm{H}}\mathbf{R}^{(\Theta)}_{\mathbf{ss}}(p_n^{(\Theta)})\mathbf{w}}{\mathbf{w}^{\mathrm{H}}(\mathbf{R}^{(\Theta)}_{\mathrm{int}}(p_n^{(\Theta)}) + \sigma^2\mathbf{I})\mathbf{w}}. \tag{25}$$

Since typically $N_{\mathrm{UT}} \ll N_{\mathrm{MC}}$, Equation (25) turns out to be an efficient way

to compute the SINR average. Figure 3 shows the comparison between N_{UT} and N_{MC} for the 3 and 5-point UT and N_{MC} ranging from 10^2 to 10^5 realizations.

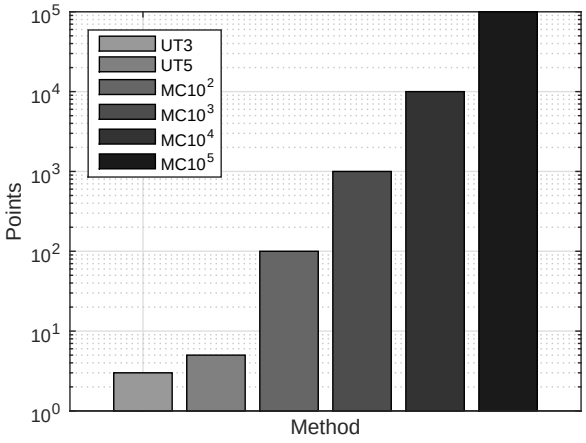

Figure 3: Number of generated random samples

4.2. *Multivariate case: Evaluating the SINR under antenna element positioning error*

In this section we consider the case where a beamforming system is perturbed by an antenna element positioning error. Since the perturbation occurs independently in each element, we now need to consider a multivariate case. The traditional Monte Carlo method consists of taking the mean after N realizations of the random vector $\boldsymbol{\mathcal{D}}$ yielding

$$\overline{\mathrm{SINR}}_{\mathrm{MC}}^{(\boldsymbol{\mathcal{D}})} = \frac{1}{N}\sum_{n}^{N} \frac{\mathbf{w}^{\mathrm{H}}\mathbf{R}_{\mathbf{ss}}^{(\boldsymbol{\mathcal{D}})}(\boldsymbol{\mathcal{D}}[n])\mathbf{w}}{\mathbf{w}^{\mathrm{H}}\left(\mathbf{R}_{\mathrm{int}}^{(\boldsymbol{\mathcal{D}})}(\boldsymbol{\mathcal{D}}[n]) + \sigma^2\mathbf{I}\right)\mathbf{w}}. \tag{26}$$

In a similar manner as in (23) and (24), the SOI and interference correlation matrices in the presence of element positioning perturbations are written as:

$$\mathbf{R}_{\mathbf{ss}}^{(\boldsymbol{\mathcal{D}})}(\boldsymbol{\mathcal{D}}[n]) = \mathbf{a}^{(\boldsymbol{\mathcal{D}}[n])}(\theta_0,\phi_0)[\mathbf{a}^{(\boldsymbol{\mathcal{D}}[n])}(\theta_0,\phi_0)]^{\mathrm{H}}, \tag{27}$$

$$\mathbf{R}_{\mathrm{int}}^{(\boldsymbol{\mathcal{D}})}(\boldsymbol{\mathcal{D}}[n]) = \sum_{i\neq 0}\mathbf{a}^{(\boldsymbol{\mathcal{D}}[n])}(\theta_i,\phi_i)[\mathbf{a}^{(\boldsymbol{\mathcal{D}}[n])}(\theta_i,\phi_i)]^{\mathrm{H}}. \tag{28}$$

By analyzing Equation (18) to find a UT equivalent for (26), we see that a sum over all random variables is needed. Therefore, we end with a sum over the three dimension for each antenna element

$$\overline{\mathrm{SINR}}_{\mathrm{UT}}^{(\boldsymbol{\mathcal{D}})} = \sum_{n_{x,1}=1}^{N_{\mathrm{UT}}} \sum_{n_{y,1}=1}^{N_{\mathrm{UT}}} \sum_{n_{z,1}=1}^{N_{\mathrm{UT}}} \sum_{n_{x,2}=1}^{N_{\mathrm{UT}}} \cdots \sum_{n_{z,M}=1}^{N_{\mathrm{UT}}} \omega_{n_{x,1}} \omega_{n_{y,1}} \omega_{n_{z,1}} \omega_{n_{x,2}} \cdots \omega_{n_{z,M}} \cdot \frac{\mathbf{w}^{\mathrm{H}} \mathbf{R}_{\mathbf{ss}}^{(\boldsymbol{\mathcal{D}})}(\mathbf{p}_{n_{x,1},\ldots,n_{z,M}}) \mathbf{w}}{\mathbf{w}^{\mathrm{H}} \left(\mathbf{R}_{\mathrm{int}}^{(\boldsymbol{\mathcal{D}})}(\mathbf{p}_{n_{x,1},\ldots,n_{z,M}}) + \sigma^2 \mathbf{I} \right) \mathbf{w}}, \tag{29}$$

where $\mathbf{p}_{n_{x,1},\ldots,n_{z,M}} = [p_{n_{x,1}}, p_{n_{y,1}}, p_{n_{z,1}}, p_{n_{x,2}} \cdots, p_{n_{z,M}}]^{\mathrm{T}}$.

Even though Gaussian distributions have non-zero tails, the actual generation of very large or very small numbers is unlikely. This work, as in common practice [21, 22], uses Gaussian distributions to model the array elements positioning errors in order to simplify the UT validation while making very little to no comprimise to the validation process. For a theoretically more precise distribution, the reader is referred to the circular normal distribution, also known as the Von Mises distribution [23]. The characteristic of a Gaussian distribution allows us to simplify (29) by considering $\mathcal{D}_x$, $\mathcal{D}_y$ and $\mathcal{D}_z$ as zero mean Gaussian random variables with variance σ_d^2. Since the sum of Gaussian random variables results in a Gaussian distribution with variance equals to the sum of the original variances [17], we can write simplified perturbed phase delays

$$\mu_{m,i}^{(\mathcal{D})} = (m-1) d \cos\theta_i \cos\phi_i + \mathcal{D}_m, \tag{30}$$

where $\mathcal{D}_m \sim \mathcal{N}\left(0, \sigma_{\mathcal{D}}^2\right)$. The total variance $\sigma_{\mathcal{D}}^2 = \sigma_d^2 \left(\cos^2\theta_i \cos^2\phi_i + \sin^2\theta_i \cos^2\phi_i + \sin^2\phi_i\right)$ is actually equal to σ_d^2, given that the sum inside the parenthesis is equal to 1 after the use of trigonometric identities. Therefore, the mean SINR com-

puted via the UT for a perturbed element positioning can be simplified to

$$\overline{\mathrm{SINR}}_{\mathrm{UT}}^{(\boldsymbol{\mathcal{D}})} = \sum_{n_1=1}^{N_{\mathrm{UT}}} \sum_{n_2=1}^{N_{\mathrm{UT}}} \cdots \sum_{n_M=1}^{N_{\mathrm{UT}}} \omega_{n_1}\omega_{n_2}\ldots\omega_{n_M} \cdot \frac{\mathbf{w}^{\mathrm{H}}\mathbf{R}_{\mathbf{ss}}^{(\boldsymbol{\mathcal{D}})}(\mathbf{p}_{n_1,n_2,\ldots,n_M})\mathbf{w}}{\mathbf{w}^{\mathrm{H}}(\mathbf{R}_{\mathrm{int}}^{(\boldsymbol{\mathcal{D}})}(\mathbf{p}_{n_1,n_2,\ldots,n_M}) + \sigma^2\mathbf{I})\mathbf{w}}. \tag{31}$$

In the multivariate case, the amount of points to be averaged by the UT varies not only with the amount of sigma points, but also with the amount of antenna elements. The comparison between the number of points needed for the MC and UT averages are shown in Figure 4.

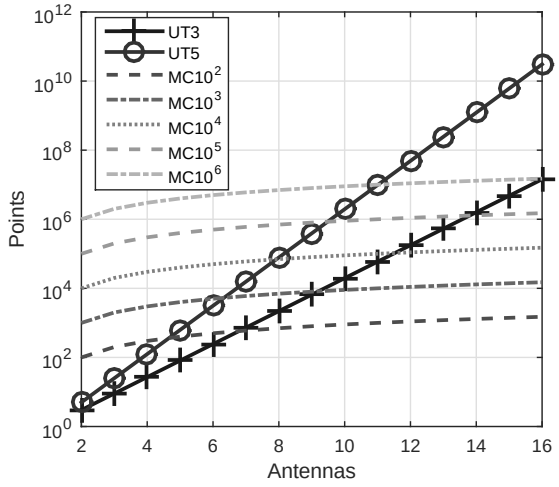

Figure 4: Comparison between the number of points generated by MC and the UT with a varying number of array elements

The total number of points computed by the UT grows exponentially in a N_{UT}^M manner while the MC has a linear growth. However, the UT can be advantageous since MC simulations may require millions of randomly generated points. In Figure 4, we see that the usage of the 3-point UT can be advantageous for up to 15 antennas if compared to 10^6 generated positions in a MC fashion. The same is true for 10 antenna elements in the 5-point UT case.

5. Simulation Results

In Section 4, we showed how the $\overline{\text{SINR}}$ is computed using the UT and the number of points needed for both MC and the UT simulations. In this section, we simulate and show the SINR averages.

One fundamental question that arises from figures 3 and 4 in Section 4 is: over how many points do we need to compute MC mean? The answer is not straight forward. The number of MC simulations has a direct impact on the precision of the mean, i.e. how close the sample mean is to the ground truth. The ground truth is hard to compute and, in this case, not known. Therefore, we cannot verify the achieved precision. However, we may consider the error of the computed mean as a random variable that also has an associated variance and, of course, the smaller the variance, the better is the estimate.

To illustrate the statement above, the light gray line in Figure 5 shows the change in the sample variance of the SINR mean from Equation (22) after 100 samples for a varying number of trials. The scenario is the same using 5 antennas

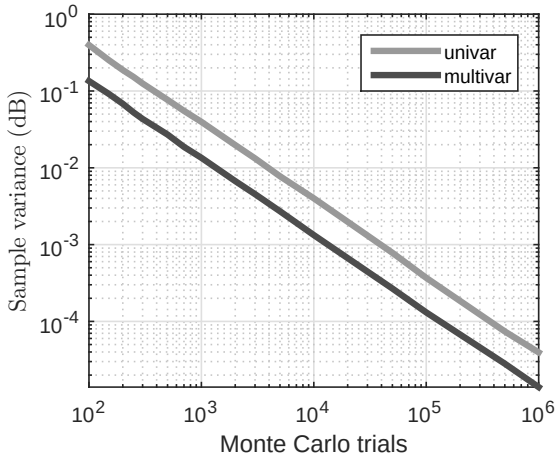

Figure 5: Sample variance versus the number of trials in Monte Carlo simulations

as described further in this section. In Figure 5, we see that a few tenths of thousands of trials are needed so that the variance is bellow 10^{-3} dB, i.e. small in comparison to the 10 dB SINR range that is shown in Section 5. The dark

line in Figure 5 shows the result for the multivariate case of Equation (26). The result shows that the variance is slightly lower for the multivariate case, as te number of points increases. Therefore, by inspection of Figure 5, we consider that the variance needed to accomplish a reasonable precision is at least one thousandth of the range in investigation, in this case, 10^{-3} dB.

For the simulations we consider 5 antenna elements and 2 impinging signals, one SOI at 90° and two interfering signals at 65° and 117°, respectively. We then vary the DOAs and take the SINR mean using the 3 and 5-point UT and 5 and 10^6 MC realizations. The results are shown in Figure 6. In order to

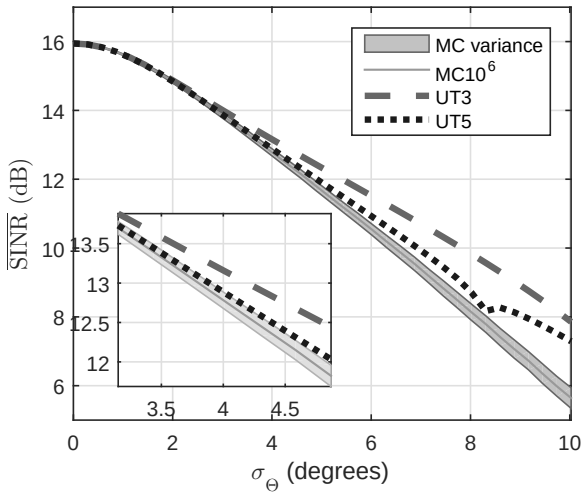

Figure 6: $\overline{\text{SINR}}$ vs σ_Θ due to DOA estimation error

guarantee a precise estimate of the mean and after inspecting Figure 5, 10^6 MC realizations are used as a reference. From Figure 6 we see that the $\overline{\text{SINR}}$ estimated using the 3-point UT follows almost exactly the 10^6 MC realizations $\overline{\text{SINR}}$ for up to 3° of standard deviation. The same holds for the 5-point UT for up to $\sigma_\Theta = 4°$. To get a better estimation more points are needed, however, a standard deviation of 4° is already a large value for most applications. We should also remind that the UT computations are done with a small fraction of the computational cost of the MC simulations.

For our simulations we assume that the mean over 10^6 MC realizations, represented by $\overline{\text{SINR}}_{\text{MC}10^6}$, is very close to the ground truth mean. Therefore, our proposed methods error is defined as

$$\text{Error} = |\overline{\text{SINR}} - \overline{\text{SINR}}_{\text{MC}10^6}|. \tag{32}$$

Equation (32) is used in sections 5.1 and 5.2 for the validation of the proposed UT-based methods.

In Subsection 5.1 we evaluate the SINR, error and computational time of the univariate UT. In Subsection 5.2, the SINR, error and computational time are evaluated for the multivariate case.

5.1. Performance Evaluation of the Univariate UT

In Figure 6 the region between the average SINR and the variance of the estimation is also shown by the shaded area. The variance was estimated for 100 trials of 10^5 generated points, where the mean over the 100 trials gives the final 10^6 points average. The shaded region gives a degree of confidence in the estimated MC. At the bottom-left corner, the graphic is zoomed in the region where the UT5 leaves the region of confidence around 4°.

Figure 7 shows the relative error between the UTs and the reference MC simulation after 10^6 realizations. From Figure 7 we see that the 5-point UT still follows the MC10^6 $\overline{\text{SINR}}$ up to $\sigma_\Theta = 6°$ with a less than 0.5 dB error margin. It is also worth noting that the error does not grow monotonically, however, the growth trend can be clearly seen. In [8], σ_Θ is varied up to 2.63° using 1000 MC trials. In Figure 7, we see that the UT5 give practically zero error up to this level, therefore, the 5-point UT can be used to compute the $\overline{\text{SINR}}$.

We then fix the standard deviation in two values $\sigma_\Theta = \{1, 6\}°$ and vary the SNR as shown in Figure 8. The darker plots show the $\overline{\text{SINR}}$ for $\sigma_\Theta = 1°$ and the brighter ones are for $\sigma_\Theta = 6°$. For a small standard deviation both UTs follow the MC simulation exactly. For a larger deviation, the UT fits the MC $\overline{\text{SINR}}$ up to an SNR of 2 dB for the 3-point UT and 8 dB for the 5-point UT. The

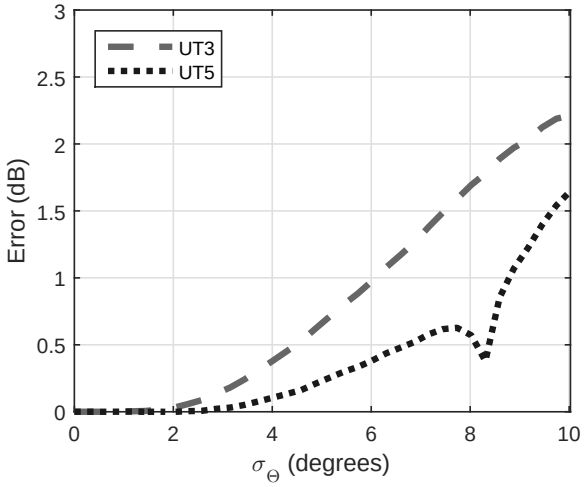

Figure 7: Error vs σ_Θ due to DOA estimation errors

reason is that for low SNRs, the noise variance on the denominator of equations (22), (25), (26) and (31) is greater than the other terms impact on the SINR than the error due to DOA estimation.

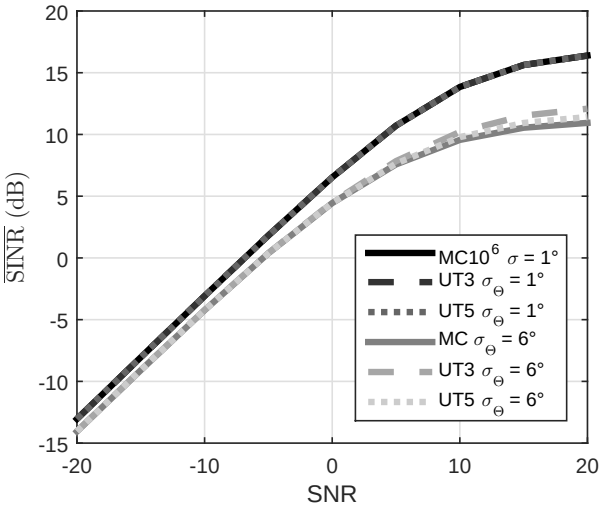

Figure 8: $\overline{\text{SINR}}$ vs SNR with fixed $\sigma_\Theta = \{2, 10\}°$

220

In the next simulation computational time is assessed and the results

are shown in Figure 9. We compare the 3-point UT and the 5-point UT with a varying number of MC trials. The results show that the 3-point UT and the 5-point UT have a low computational time in comparison to the MC simulations even when only tens of trials are performed. We can clearly see that these results are tied to the number of points generated as shown in Figure 3.

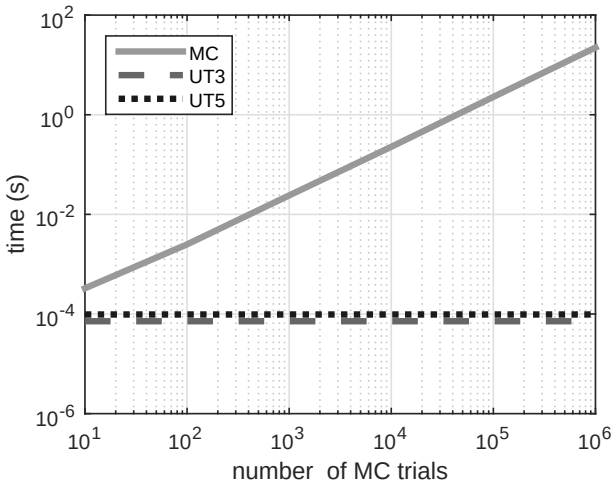

Figure 9: Computational time of the univariate UT in the presence of DOA estimation error

5.2. Performance Evaluation of the Multivariate UT

In Figure 10 we simulate the multivariate case with fixed SINR and a varying $\sigma_{\mathcal{D}}$ for random element positions. Again, the SINRs are averaged using the 3-point UT follow the MC curve very closely for small deviations. For larger deviations, the 5-point UT fits the MC $\overline{\text{SINR}}$. Such large deviations are, however, improbable to occur in an array manufacturing process. In case the deviation is large, e.g. cooperative array, the MC curve can be followed further by increasing the number of points, although care should be taken due to the rapid increase in complexity in multivariate scenarios (see Figure 4). For comparison, we use a comparable computational complexity from Figure 4. As in Figure 6, the region between the variances is shaded. Also, the the zoomed curves are shown in

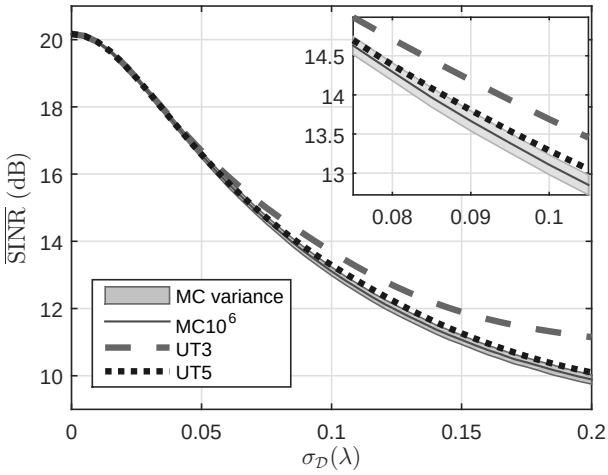

Figure 10: $\overline{\text{SINR}}$ vs $\sigma_{\mathcal{D}}$ due to array element positioning imperfections

the top-right corner focusing the point where the UT5 leaves the shaded region around 0.09 λ.

Figure 11 shows the error for the multivariate case. From Figure 11 we see that the error is virtually zero for the 3 and 5-point UT with a standard deviation of up to 0.03 and 0.05, respectively. Also, the 3-point UT error grows faster than te 5-point UT. Similarly as in the previous scenario, one may not expect a monotonic growth in the error computation for a increasing $\sigma_{\mathcal{D}}$. The error for the 625 realizations SINR average varies largely. Therefore, it is not possible to conclude the error levels.

In Figure 12, the standard deviation $\sigma_{\mathcal{D}}$ is fixed to $\{0.03, 0.12\}$ and the SNR is varied. Similarly as in the univariate case, the UT3 and UT5 $\overline{\text{SINR}}$s follow the MC SINR average. When the noise is low and the positioning error is high, the UT $\overline{\text{SINR}}$s deviate from the MC mean. However, this deviation is small and the positioning error is high most of the practical applications.

The final simulation assesses the computational time of the multivariate UT and the results are show in Figure 13. We compare the 3-point UT and the 5-point UT with a varying number of MC trials. The results show that the 3-point UT has a low computational time in comparison to the MC simulations when

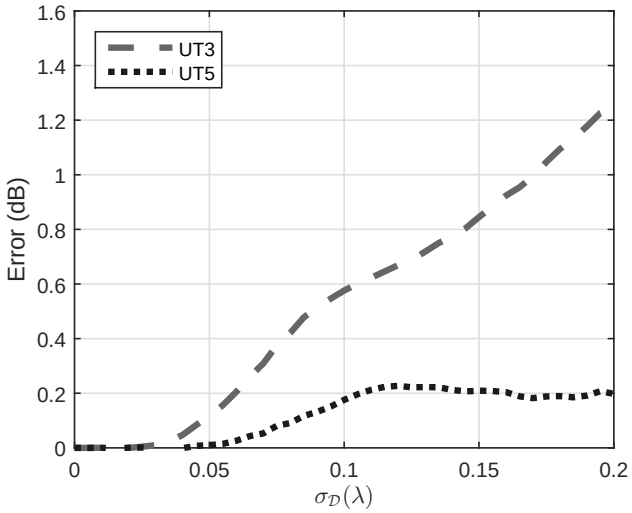

Figure 11: Error versus $\sigma_{\mathcal{D}}$ due to array element positioning imperfections

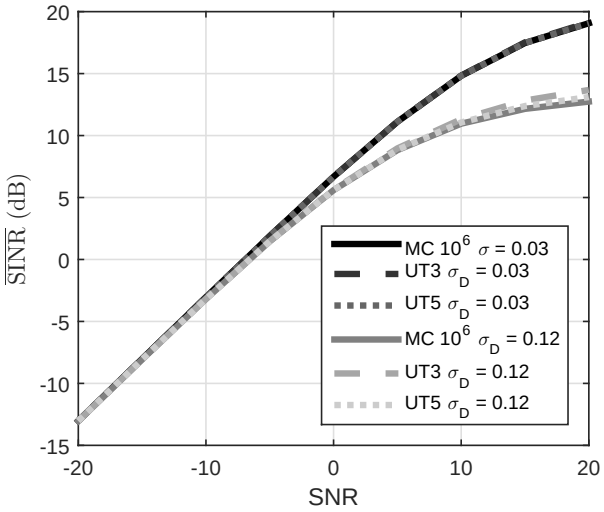

Figure 12: $\overline{\text{SINR}}$ vs SNR with fixed $\sigma_{\mathcal{D}} = \{0.03, 0.12\}$

roughly more than 100 MC trials are needed. The 5-point UT is advantageous from the computational point of view when roughly more than 1000 MC trials are required. This result is in accordance with the number of points that need to be generated for the UT and MC simulations as shown in Figure 4.

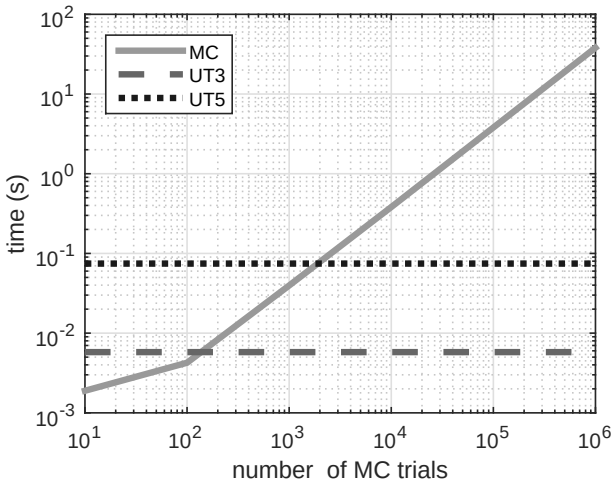

Figure 13: Computational time of the multivariate UT in the case of element positioning pertubations

6. Conclusion

This work shows a novel method using the UT for assessing the SINR average of a beamformer. We show that the computational burden of the evaluation of a beamformer can be greatly reduced while maintaining the reliability of the simulations. We chose the DOA estimation error and imperfections of the array elements positions to assess the SINR average of a DS beamformer using the proposed method and compared with the traditional MC simulations. The simulations shows that the UT is very reliable even only 5 points are computed for small to medium error.

Acknowledgments

The authors would like to thank the Coordenação de Aperfeiçoamento de Pessoal de Nível Superior (CAPES) under the PVE grant number 88881.030392/2013-01, the productivity grant number 303905/2014-0, the postdoctoral scholarship abroad (PDE) number 207644/2015-2, the joint double degree scholarship number 88887.115692/2016-00 and the Program Science without Borders-

Aerospace Technology supported by CNPq and CAPES for the postdoctoral scholarship abroad (PDE) number 207644/2015-2.

References

[1] W. Herbordt and W. Kellermann, “Adaptive beamforming for audio signal acquisition,” Springer, pp. 155-194, 2003.

[2] L. J. Ziomek, “Fundamentals of Acoustic Field Theory and Space-Time Signal Processing,” CRCPress, 1995.

[3] S. M. Alamouti, “A simple transmit diversity technique for wireless communications,” IEEE Journal on Selected Areas in Communications, vol. 16, Issue 8, pp. 1451-1458, Oct. 1998.

[4] Z. Yang, R.C. de Lamare, and X. Li, “L1 regularized STAP algorithm with a generalized sidelobe canceler architecture for airborne RADAR,” 2011 IEEE Statistical Signal Processing Workshop, pp. 329-332, Jun. 2011.

[5] B. D. van Veen e K. M. Buckley, “Beamforming: a versatile approach to spatial filtering,” ASSP Magazine IEEE, vol. 5 , Issue 2, pp. 4-24, Abr. 1988.

[6] H. Krim, M. Viberg, “Two decades of array signal processing research: the parametric approach,” IEEE Signal Processing Magazine, vol. 13, Issue 4, pp. 67-94, 1996.

[7] J. A. Gubner, “Probability and Random Processes for Electrical end Computer Engineers,” 1st ed. Cambridge University Press, 2006, iSBN: 978-0-521-86470-1.

[8] W. Liu, S. Ding, M. Jin, J. Kim, “A Robust DOA/Beamforming Algorithm Using the Constant Modulus Feature,” International Journal of Innovative Computing, Information and Control, v. 8, n. 3(B), March 2012.

[9] J. J. Blanz, A. Papathanassiou, M. Haardt, I. FuriÃş, P. W. Baier, “Smart Antennas for Combined DOA and Joint Channel Estimation in Time-Slotted

CDMA Mobile Radio Systems with Joint Detection," IEEE Trans. on Vehicular Technology, vol. 49, no. 2, pp. 293-306, Mar. 2000.

[10] M. V. Woodward and P. J. Mosterman,"Challenges for embedded software development," in IEEE International Midwest Symposium on Circuits and Systems, Aug 2007.

[11] F. Roemer, M. Haardt, and G. Del Galdo, "Analytical performance assessment of multi-dimensional matrix- and tensor-based ESPRIT-type algorithms," IEEE Transactions on Signal Processing, vol. 62, pp. 2611-2625, May 2014.

[12] F. Li, H. Liu, and R. J. Vaccaro, "Performance analysis for DOA estimation algorithms: Unification, simplifications, observations," IEEE Trans. Aerosp. Electron. Syst. , vol. 29, no. 4, pp. 1170-1184, Oct. 1993.

[13] S. J. Julier, J. K. Uhlmann,"A General Method for Approximating Nonlinear Transformations of Probability Distributions," Technical report, RRG, Dept. of Eng. Science, Univ. of Oxford, 1996.

[14] M. A. M. Marinho, J. P. C. L. da Costa, F. Antreich and L. R. A. X. de Menezes, "Unscented transformation based array interpolation," in Proc. 40th International Conference on Acoustics, Speech, and Signal Processing (ICASSP), Brisbane, Australia, April 2015.

[15] I. Arasaratnam, S. Haykin, Cubature Kalman Filters, IEEE Transactions on Automatic Control, vol. 54, no. 6, June 2009.

[16] S. J. Julier, J. K. Uhlmann,"Unscented Filtering and Nonlinear Estimation,", Proceedings of the IEEE, vol. 92, no. 3, pp. 401-422 Mar. 2004.

[17] A. Papoulis, "Probability, Random Variables, and Stochastic Processes," 3rd ed. New York: McGraw-Hill, 1991.

[18] L. R. A. X. de Menezes, A. Ajayi, C. Christopoulos, P. Sewell, G. A. Borges, "Extracting Statistical Moments of Output Quantities from a Small Number

of Time-Domain Simulations," Workshop on Computational Electromagnetics in Time-Domain, CEM-TD 2007, 2007.

[19] L. R. A. X. de Menezes, E. A. Jr, M. N. de Sousa, and G. A. Borges, "Estimation of the Probability Density Function in Electromagnetic Propagation Problems with the Unscented Transform and TLM," Proceedings of The 24th Annual Review of Progress in Applied Computational Electromagnetics, 2008.

[20] L. C. Godaram, "Application of Antenna Arrays to Mobile Communications, Part II: Beamforming and Direction-of-Arrival Considerations." Proceedings of the IEEE, Vol. 85, No. 8, pp. 1195-1245, Aug. 1997.

[21] B. P. Flanagan, K. L. Bell, "Improved array self calibration with large sensor position errors for closely spaced sources," Proceedings of the 2000 IEEE Sensor Array and Multichannel Signal Processing Workshop, pp. 484-488, 2000.

[22] J.-H. Lee, C.-C. Wang, "Adaptive Array Beamforming with Robust Capabilities under Random Sensor Position Errors," Proceedings of IEE Radar Sonar Navigation, v. 152, no. 6, Dec. 2005.

[23] G. W. Hill, "Algorithm 518: Incomplete Bessel Function I0. The Von Mises Distribution," ACM Transactions on Mathematical Software (TOMS), v. 3, no. 3, Sept. 1977.

Vitae

Ricardo Kehrle Miranda received the Diploma degree in telecommunications engineering in 2010 and the M.Sc. degree in electronic and automation systems in 2013 both from the University of Brasília (UnB), Brazil. In Germany, he did part of his M.Sc. work at the University of Erlangen-Nuremberg in 2012 and was as visitor student at the German Aerospace Center (DLR) in February and March of 2014. In Japan, he was an intern in the space industry

for 8 months in a partnership with the Wakayma University, the Tokyo University and the Brazilian Aerospace Agency. Currently, he pursues a double Ph.D. degree at both the UnB and the TU Ilmenau with interests on array signal processing, multilinear algebra and space communications.

João Paulo C. L. da Costa received the Diploma degree in electronic engineering in 2003 from the Military Institute of Engineering (IME) in Rio de Janeiro, Brazil, his M.Sc. degree in telecommunications in 2006 from University of Brasília (UnB) in Brazil, and his Doktor-Ingenieur (Ph.D.) degree in electrical engineering and information technology with Magna cum Laude in 2010 from Ilmenau University of Technology (TU Ilmenau) in Germany. During his Ph.D. studies, he was a scholarship holder of the National Counsel of Technological and Scientific Development (Conselho Nacional de Desenvolvimento Científico e Tecnológico, CNPq) of the Brazilian Government and also a captain of the Brazilian Army. He has published more than 50 papers in refereed journals and conference proceedings and received three conference Best Paper awards at the International Congress on Ultra Modern Telecommunications and Control Systems (ICUMT'12) and the international conference on forensic computer science (ICoFCS'12 and ICoFCS'13). He has been visiting professor at University of Erlangen-Nuremberg, Munich Technical University, University of Seville and Harvard University. Currently, he is a professor at the Department of Electrical Engineering, University of Brasília (UnB). He is a member of the Graduate Program in Electrical Engineering (PPGEE), of the Laboratory of Automation and Robotics (LARA) and of the Microwave and Wireless Research Group (MWSL) at UnB. He is responsible for the Laboratory of Array Signal Processing (LASP) at UnB. His research interests are in the areas of multidimensional array signal processing, MIMO communication systems, microphone array signal processing, multi-linear algebra, principal component analysis (PCA), and model order selection

Florian Roemer studied computer engineering at the Ilmenau University of Technology, Germany, and McMaster University, Hamilton, ON, Canada. He received the Diplom-Ingenieur degree in communications engineering and the

doctoral (Dr.-Ing.) degree in electrical engineering from the Ilmenau University of Technology in October 2006 and October 2012, respectively. From December 2006 until September 2012, he was a Research Assistant in the Communications Research Laboratory at Ilmenau University of Technology. In October 2012 he joined the Digital Broadcasting Research Group, a joint research activity between the Fraunhofer Institute for Integrated Circuits IIS and Ilmenau University of Technology, as a postdoctoral research fellow. His research interests include multi-dimensional signal processing, high-resolution parameter estimation, MIMO communications as well as compressive sensing. For his diploma thesis, Mr. Roemer received the Siemens Communications Academic Award in 2006 and for his dissertation, the best dissertation award from the FÃűrder- und Freundeskreis (FFK) of the Ilmenau University of Technology in 2013 as well as the EURASIP best PhD award in 2016. He has also served as a member of the organizing committee of the 19th International Workshop on Smart Antennas (WSA) 2015 in Ilmenau, Germany.

Leonardo R. A. X. de Menezes received his BS and MS degrees in Electrical Engineering from the Universidade de Brasilia, Brazil, in 1990 and 1993, respectively, and Ph.D. degree from the University of Victoria, BC, Canada, in 1996. He is currently an associate professor in the Department of Electrical Engineering, University of Brasilia. His research interests are in numerical modeling, electromagnetic theory, mobile systems, and software radio.

Giovanni Del Galdo was born in 1977 in Merano, Italy. He studied telecommunications engineering at Politecnico di Milano and received his Master's degree in 2002. He then joined the Communications Research Laboratory at Ilmenau University of Technology (TUIL), where he received his doctoral degree in 2007 on the topic of channel modeling for MIMO wireless communication systems. He has been a Full Professor in the Department of Electrical Engineering and Information Technology and Head of the DVT Research Group at Ilmenau University of Technology since 2012. Shortly thereafter, he joined the Fraunhofer Institute for Integrated Circuits IIS and the International Audio Laboratories Erlangen as senior scientist. Here, he worked on audio watermark-

ing, parametric representations of spatial sound, and sound field analysis via microphone arrays. In 2012 he was appointed full professor at TUIL as head of the DVT Research Group, a joint activity between TUIL and Fraunhofer IIS on the research area of wireless distribution systems and digital broadcasting. The group manages and develops the Fraunhofer IIS Facility for Over-the-air Research and Testing (FORTE) further. His current research interests include the analysis, modeling, and manipulation of multi-dimensional signals, over-the-air testing for terrestrial and satellite communication systems, and sparsity promoting reconstruction methods.

André L. F. de Almeida received the B.Sc. and M.Sc. degrees in electrical engineering from the Federal University of Ceará, Brazil, in 2001 and 2003, respectively, and the double Ph.D. degree in Sciences and Teleinformatics Engineering from the University of Nice, Sophia Antipolis, France, and the Federal University of Ceará, Fortaleza, Brazil, in 2007. He is currently an Assistant Professor with the Department of Teleinformatics Engineering of the Federal University of Ceará. During fall 2002, he was a visiting researcher at Ericsson Research Labs, Stockholm, Sweden. From 2007 to 2008, he held a one year research position at the I3S Laboratory, CNRS, France. In 2008, he was awarded a CAPES/COFECUB research fellowship with the I3S Laboratory, CNRS, France. In 2010, he was appointed a productivity research fellow from CNPq (the Brazilian National Council for Scientific and Technological Development). In the spring 2012, he was a visiting professor at the University of Nice Sophia-Antipolis, France. He is affiliated to the IEEE Signal Processing for Communications and Networking (SPCOM) Technical Committee of the IEEE Signal Processing Society. He serves as an Associate Editor of the IEEE Transactions on Signal Processing, Circuits, Systems & Signal Processing, and the KSII Transactions on Internet and Information Systems. His research interests lie in the area of signal processing for communications, and include blind identification, source separation, MIMO systems, tensor decompositions and multilinear algebra applied to communications and data analysis.